Development of an Anthropomorphic Prosthetic Hand with Underactuated Mechanism

Wooseok Ryu [1], **Youngjin Choi [2]**, **Yong Je Choi [1]**, **Yeong Geol Lee [1]** and **Sungon Lee [2],***

[1] Department of Mechanical Engineering, Yonsei University, Seoul 03722, Korea; fbdntjr3@gmail.com (W.R.); yjchoi@yonsei.ac.kr (Y.J.C.); yngeolee@yonsei.ac.kr (Y.G.L.)

[2] School of Electrical and Engineering, Hanyang University, Ansan 15588, Korea; cyj@hanyang.ac.kr

* Correspondence: sungon@hanyang.ac.kr; Tel.: +82-31-400-5174

Featured Application: We developed an anthropomorphic prosthetic hand with an underactuated mechanism for wrist or forearm amputees. The fabricated prototype is 475 g and can realize self-adaptive grasping, adduction/abduction, and flexion/extension motions.

Abstract: An anthropomorphic prosthetic hand for wrist or forearm amputees is developed herein. The prosthetic hand was designed with an underactuated mechanism, which makes self-adaptive grasping possible, as well as natural motions such as flexion and extension. The finger and thumb modules were designed with four degrees of freedom by motions of the distal interphalangeal, proximal interphalangeal, and metacarpophalangeal joints. In this research, we pursued several novel trials in prosthetic hand design. By using two four-bar linkages composed of a combination of linkages and gears for coupling joints at each finger, it was possible to make a compact design, and the linkage has advantages such as accurate positioning, uniform power transmission, and high payload. Also, by using constant-velocity joints, torque is transferred to finger modules regardless of adduction/abduction motions. In addition, adduction/abduction and self-adaptive grasping motions are passively realized using torsional springs. The developed prosthetic hand was fabricated with a weight of 475 g and a human hand size of 175 mm. Experiments with diverse objects showed its good functionality.

1. Introduction

For finger and forearm amputees, prosthetic and robotic hands of different types have been developed steadily, and human hand motions, such as natural and self-adaptive grasping motions, have been realized by anthropomorphic hands with various mechanism types and designs [1,2]. For instance, the DLR hand and Robonaut hand were developed with the objective of dexterous manipulation [3,4]. Jing developed a biomimetic prosthetic hand with the aim of reducing weight and cost [5]. In addition, the i-Limb (Touch Bionics), the BeBionic hand (RSL Steeper), the Vincent hand (Vincent Systems), and the Michelangelo hand (Otto Bock) have been made available to the public [6–9].

Grasping motion is an important function of the hand, and hands with an underactuated mechanism have a remarkable ability to grasp differently shaped objects adaptively because the control of robotic hands with multiple degrees of freedom (DOFs) becomes simple. Furthermore, when hands using an underactuated mechanism are designed, the description and design to realize the desired motions according to target grasping types become easier.

In the design of an underactuated mechanism, the torque produced by actuators is transferred to each phalanx using diverse methods such as tendons, gears, and linkages. Most of the developed

underactuated hands with five fingers, e.g., the Cyber hand [10], i-Limb [6], Smart hand [11], and Toronto Bloorview Macmillan (TBM) hand [12], were designed using the tendon-driven method. This has the advantage of producing motions that are closely similar to those of the human hand using minimal parts, and the design is very simple and lightweight. However, fixing the tendons and maintaining their tension is difficult in limited space, and the slack and taut problem of tendons should be solved. Moreover, the assembly to have equal tension in each finger module is difficult, and nonuniform tension can make control difficult. Therefore, in terms of sustainability, this method has a weakness. Hands designed using gears and linkages have advantages in terms of uniform power transmission in each finger, exact position control, and high payload, even if they require more mechanical components and have a large and complex structure. In addition, research related to control contact force with objects in grasping has been performed [13,14].

In this research, the focus was on the need for the prosthetic hand to appeal to users in terms of weight and shape (anthropomorphic configuration) with high performance (accurate positioning and uniform power transmission), and we designed the underactuated hand mechanism using a combination of gears and linkages, as shown in Figure 1. Compact design in an underactuated mechanism composed of only linkages is difficult because the linkages have diverse lengths for realizing extension/flexion motions, while a mechanism using a combination of gears and linkages can be designed compactly in limited space. In addition, gear reduction ratios and metal frames can increase the available payload and strength of the mechanism. Therefore, we designed the finger module with two four-bar linkages composed of a combination of gears and linkages, and passive motions are realized by torsional springs. The distal interphalangeal (DIP), proximal interphalangeal (PIP), and metacarpophalangeal (MCP) joints are coupled by gears and four-bar linkages. The suggested hand realizes natural (extension/flexion) and self-adaptive grasping motions including adduction and abduction.
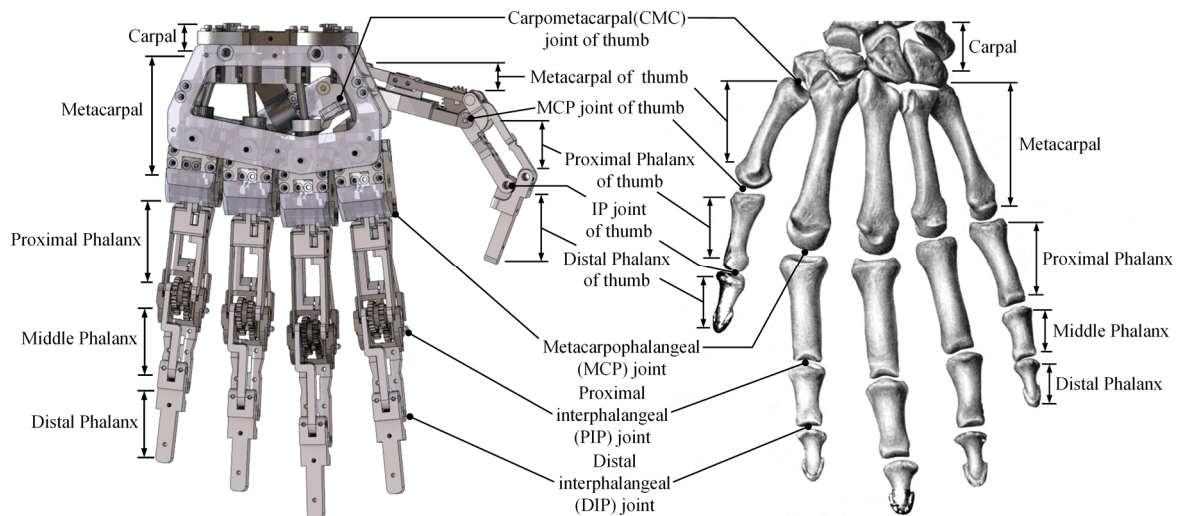

Figure 1. Skeleton structure of the human hand (right) and nomenclature of the proposed prosthetic hand (left).

This paper is organized as follows: The design and operation principles of the suggested robotic hand are described and illustrated in Section 2. In Section 3, the kinematic and finite element method (FEM) analyses are explained. Finally, in Section 4, the prototype hand is represented, and experiments are performed.

2. Design of the Hand Mechanism

2.1. Design Concepts and Desired Specifications

The grasping motions of an underactuated hand are classified into eight motions, as shown in Table 1 [15,16]. We decided that the desired hand motions are to hold objects used in daily life, such as remote controls, computer mice, paper cups, and spoons, as well as to carry bags. These desired motions are affiliated with the cylinder power, sphere power, tripod, and hook grip of the eight grasping motions. Therefore, the hand mechanism should be designed to make these motions involving natural motion to play the role of a prosthetic hand. To realize the selected grasping motions, the finger and thumb modules were designed with one active and three passive motions, which are realized by one actuator and three torsional springs in each module. In the proposed prosthetic hand, the natural motion (extension and flexion) is produced by the five actuators, and the fifth torsional springs are used for self-adaptive grasping when the surfaces of each phalanx of the finger and thumb are in contact with external objects.

Table 1. Eight grasping motions of an underactuated hand.

Cylinder Power	Sphere Power	Tip Pinch	Prismatic Pinch
Tripod	**Lateral Pinch**	**Hook Grip**	**Flat Hand**

The target weight of the prosthetic hand was set to be <500 g, suggested in [2] as a suitable weight for a prosthetic hand. The desired velocity of the fingertip was >115°/s, and the desired receptible force of the hardware in a finger module was 3 N. Moreover, the ranges of flexion/extension and adduction/abduction in the finger and thumb modules are 0–90°, 0–60°, 0–90°, and 0–20°, respectively.

2.2. Mechanism Design

Fingers are composed of two interphalangeal (IP) joints, i.e., the PIP and DIP joints, and an MCP joint, as shown in Figure 1. IP joints that make flexion and extension motions can be designed as revolute joints. Although the MCP joint in the human hand is made of a ball joint type, it was designed using two revolute joints at a right angle in this research because rotation along the length direction of the finger is almost zero. The two revolute joints produce adduction/abduction and flexion/extension. The skeleton of the thumb has two differences from those of the fingers. First, it does not have the middle phalanx (Figure 1). Therefore, the carpometacarpal (CMC) joint articulated with the carpal and metacarpal of the thumb was designed using two revolute joints at right angles. Second, in the thumb, the MCP joint was made of a revolute joint. The IP joint of the thumb was designed as a revolute joint. By designing the thumb module in the same configuration as the finger module, we have the advantage that all fingers and the thumb can be designed as identical modules.

The designed finger module consists of three sections, as shown in Figure 2a:

(1) The first section is the blue section from the metacarpal to the proximal phalanx. Proximal phalanx motion is produced from 0° to 90° in natural motion because the miter gear moves from 0° to 90° and the gear ratio is 24:24. By connecting a torsional spring between the metacarpal and an axis of the MCP joint, a passive motion that restricts 1 DOF during natural motion is performed. The available angle of the torsional spring is 40° and the angle for preload is 15°.

(2) The second section is the green section from the metacarpal to the middle phalanx. This is made of a four-bar and a torsional spring. The middle phalanx provides motion in the range from 0° to 180° in natural motion because the section has a 32:16 gear ratio. In addition, a torsional spring connects the metacarpal and an axis of the MCP joint. Therefore, a passive motion (1 DOF) is also produced in this part. The available angle and angle for preload of the torsional spring are 40° and 15°, respectively, which is the same in the blue section. In these two sections, passive motions of 2 DOFs during natural motion are restricted completely.

(3) The third section (red) is composed of two four-bar mechanisms. This section provides active motion (1 DOF) in which the distal phalanx moves between 0° and 288° because this section is connected with 32:16, 16:16, and 22:10 gear ratios.
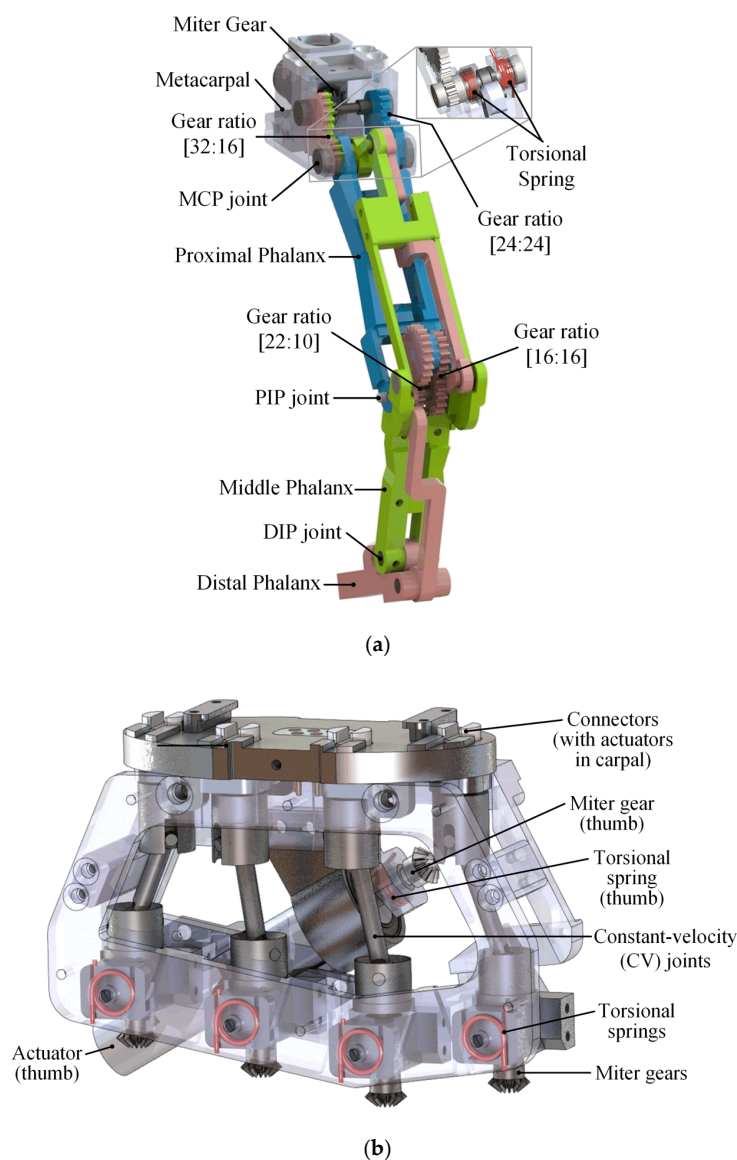

(**a**)

(**b**)

Figure 2. Constitution of (**a**) the finger module and (**b**) palm module.

The palm module includes torsional springs, an actuator for driving the thumb, and constant-velocity (CV) joints to transfer the power produced by actuators located in the carpal. There are five torsional springs. The torsional spring installed on the thumb plays a role in the rest motion of the thumb's CMC joint. The available angle and angle for the preload are 60° and 10°, respectively. The other springs were installed to realize adduction/abduction motions of the fingers, as shown in Figure 2b. The available angle of them is 20°, and the angle for preload is 10°. The directions of motions at the forefinger and the other fingers are opposing. In other words, the adduction/abduction motions of the forefinger are rotated in the clockwise direction, while these motions of the other fingers are rotated in the counterclockwise direction. By connecting actuators in the carpal and the miter gears of each finger using the CV joint, the velocity and position of the miter gear have the same values as those of the actuators. Moreover, the CV joints can transfer the power from actuator to miter gear regardless of adduction/abduction in the MCP joint.

2.3. Operation Principles

A schematic of the structure of the finger module is depicted in Figure 3. O, O′, and O″ are along the same axis, which is fixed on the ground.
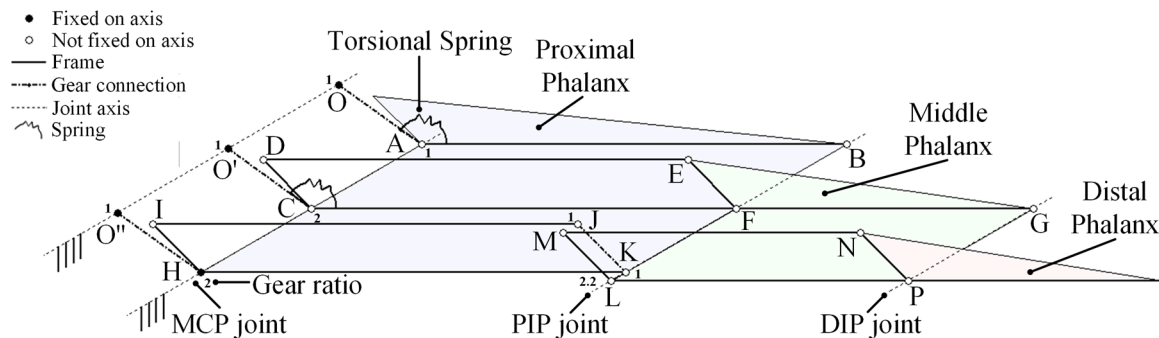

Figure 3. Schematic of the structure of the finger module.

$\overline{OA}$, $\overline{O'C}$, and $\overline{O''H}$ are connected by gears with gear ratios of 1:1, 1:2, and 1:2, respectively. The three divided sections in Figure 3 are the same as the three sections depicted in Figure 2a. In natural motion, the proximal phalanx rotates as much as the actuated motion and the middle phalanx moves 2 times more than the actuated angle, as shown in Figure 4a, because these two phalanges have preload forces from torsional springs. In the case of the middle phalanx, the output motion is transmitted through a four-bar mechanism, i.e., R_{CDEF} when R_{abcd} means a four-bar linkage composed of points a, b, c, and d in Figure 3. The distal phalanx is moved 3.2 times more than the original angle from the actuator because the distal phalanx is connected to two four-bar mechanisms (R_{HIJK} and R_{LMNP} in Figure 3), and the gear ratios are 1:2 and 1:2.2, respectively. If contact forces are produced on the proximal phalanx or the middle phalanx by external forces, two phalanges stop at the contact positions, as shown in Figure 4b. Then, the gears connected to A, C, and H proportionally rotate continually with the actuated angle, and the torsional springs are compressed gradually in self-adaptive grasping motion. Finally, the finger has the configuration that all phalanges are in contact with the object.
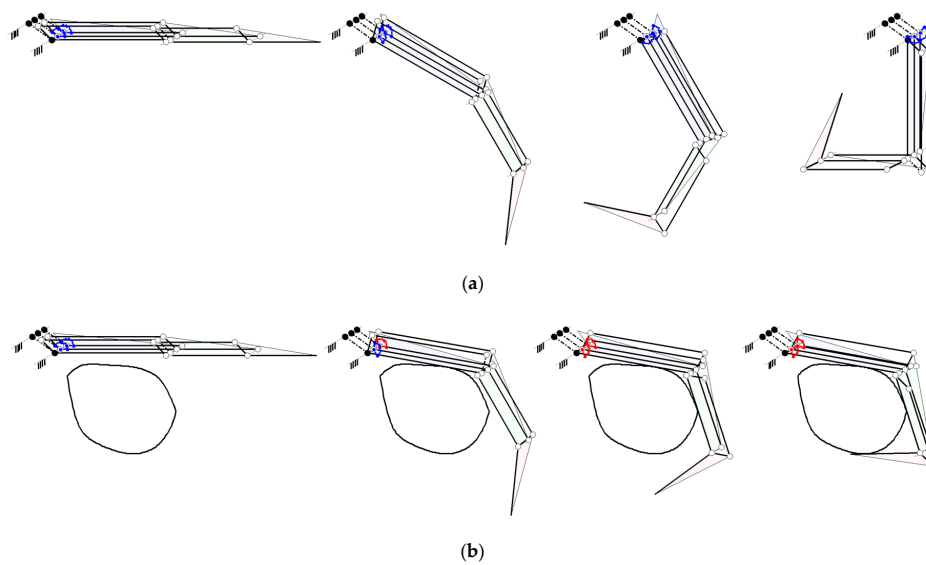
(a)

(b)

Figure 4. (**a**) Natural motion and (**b**) self-adaptive grasping motion of the proposed finger: blue and red color springs represent springs uncompressed and compressed by external forces, respectively.

3. Analysis of The Finger Module

3.1. Kinematic Analysis

In the proposed finger module, the lengths of the cross links in each four-bar mechanism are equal. The kinematic model of the robotic hand is represented in Figure 5. The fixed reference frame $O(x, y)$ was assigned at the base axis. θ_B is the actuated angle, and θ_P, θ_M, and θ_D are the rotated angles of the proximal phalanx, middle phalanx, and distal phalanx, respectively. When the rotation angle from an actuator is given, the positions (P_B, P_G, and P_Q) of the phalanxes can be determined. P_i represents the position of point i in Figure 5.
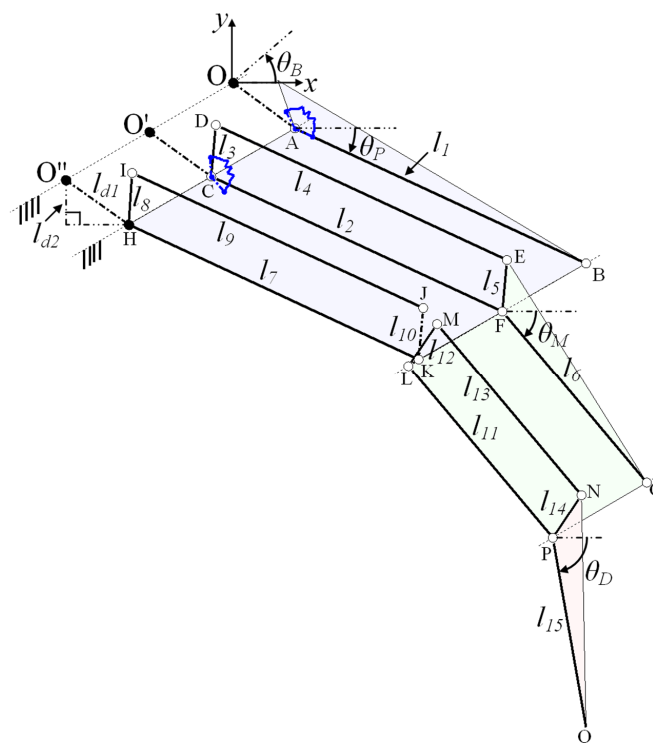

Figure 5. Kinematic parameters of the finger module.

3.1.1. Proximal Phalanx

The location of the MCP joint (P_A) is set by design variables l_{d1} and l_{d2} such that

$$P_A = P_O + \begin{bmatrix} \sqrt{l_{d1}^2 - l_{d2}^2} \\ -l_{d2} \end{bmatrix}. \tag{1}$$

The length of the proximal phalanx (l_1) is 50 mm. Therefore, the position P_B is decided by

$$P_B = P_A + \begin{bmatrix} 50 \cos \theta_P \\ -50 \sin \theta_P \end{bmatrix}. \tag{2}$$

In natural motion, θ_B is equal to θ_P.

3.1.2. Middle Phalanx

The lengths of the four-bar related to the middle phalanx are $l_2 = l_4 = 50$ mm and $l_3 = l_5 = 8$ mm. In addition, the length of the middle phalanx (l_6) is 35 mm. The position P_G is determined by

$$P_G = P_B + \begin{bmatrix} 35 \cos 2\theta_M \\ -35 \sin 2\theta_M \end{bmatrix}. \tag{3}$$

In natural motion, θ_M is also equal to θ_P.

3.1.3. Distal Phalanx

The lengths of the four-bars related to the distal phalanx are $l_7 = l_9 = 50$ mm, $l_8 = l_{10} = 8$ mm, $l_{11} = l_{13} = 35$ mm, and $l_{12} = l_{14} = 8$ mm. Finally, the length of the distal phalanx (l_{15}) is 30 mm. Therefore, the position P_Q is calculated such that

$$P_Q = P_G + \begin{bmatrix} 30 \cos 3.2\theta_D \\ -30 \sin 3.2\theta_D \end{bmatrix}. \tag{4}$$

θ_D is always equal to θ_B.

3.2. FEM Analysis

In the design of an underactuated hand mechanism using gears and linkages, the components of the hand are designed in small size. Particularly, the thicknesses of frames composing the four-bar linkages in the suggested model were designed to be thin. Thus, verification of the configuration of the design components in the desired conditions should be performed. In this section, finite element method (FEM) analysis of the finger module was performed to investigate the stress distribution and deflection. Above all, the mechanical parts such as shafts and bearings and the other components were set to stainless steel, steel, and aluminum 6061, respectively. Then, the analysis condition was given such that external force was applied along the *y*- and *x*-coordinate axes at the fingertip, respectively, as shown in Figure 6. The analysis configuration of the finger module is the shape after finishing self-adaptive grasping because the magnitude of external force applied to the finger module is the largest in this configuration. The magnitude of the applied external force is 9 N, which is the magnitude implying a safety factor of 3.

Figure 6 shows the results of the FEM analysis. Figure 6a,b represents the stress distribution and deflection, respectively, in each condition. In analyses of the stress distribution in each case, the maximum stresses are produced at the linkage frame of the four-bar in the proximal phalanx; these are represented by red arrows in Figure 6a, and the maximum stresses in each case are 54.4×10^6 N/m^2 and 157×10^6 N/m^2, respectively. Because the linkage part producing the maximum stress is fabricated

using steel and the tensile strength of steel is 620 MPa, the prosthetic hand is designed for safety and can be used with adequate rigidity in the desired conditions.

Furthermore, in Figure 6b, which is the results of the deflection analysis, the maximum deflections in the two conditions are 0.055 mm and 0.151 mm, respectively. Thus, the developed prosthetic hand can perform the desired motions suitably.
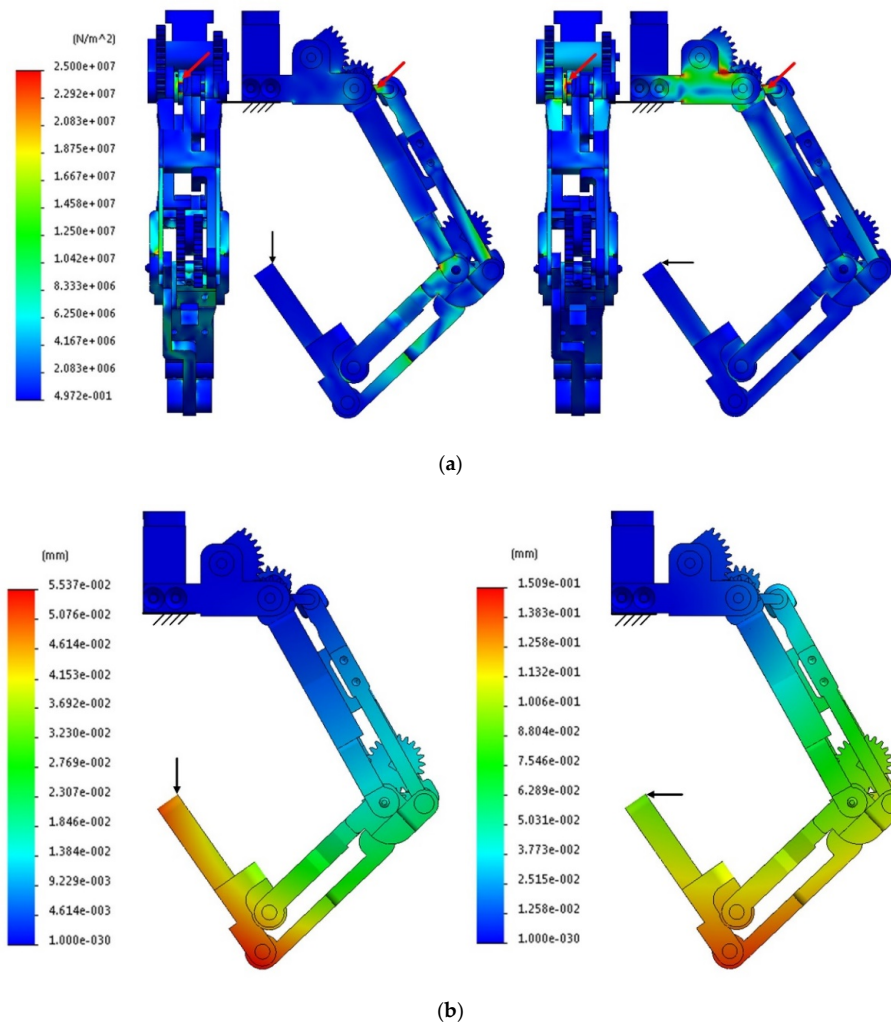

(a)

(b)

Figure 6. (**a**) Stress distributions and (**b**) deflections in the finger module when external forces are applied along the *y*- (left) and *x*-coordinate axes (right) at the fingertip.

4. Results and Discussion

4.1. Prototype

We developed a prototype of the prosthetic hand mechanism, as shown in Figure 7. The size of the hand is similar to that of a normal male human hand, as shown in Table 2. The weight including cases and actuators is about 475 g. In comparison with the existing high-end commercial prosthetic hands such as i-Limb and Bebionic, the weight of the proposed one is decreased by approximately 23% (i-Limb) and 12% (Bebionic). To improve the grasping force, cases made of rubber material were attached on parts that come into contact with an object. Moreover, we used custom-built spur gears, miter gears, CV joints, and torsional springs.
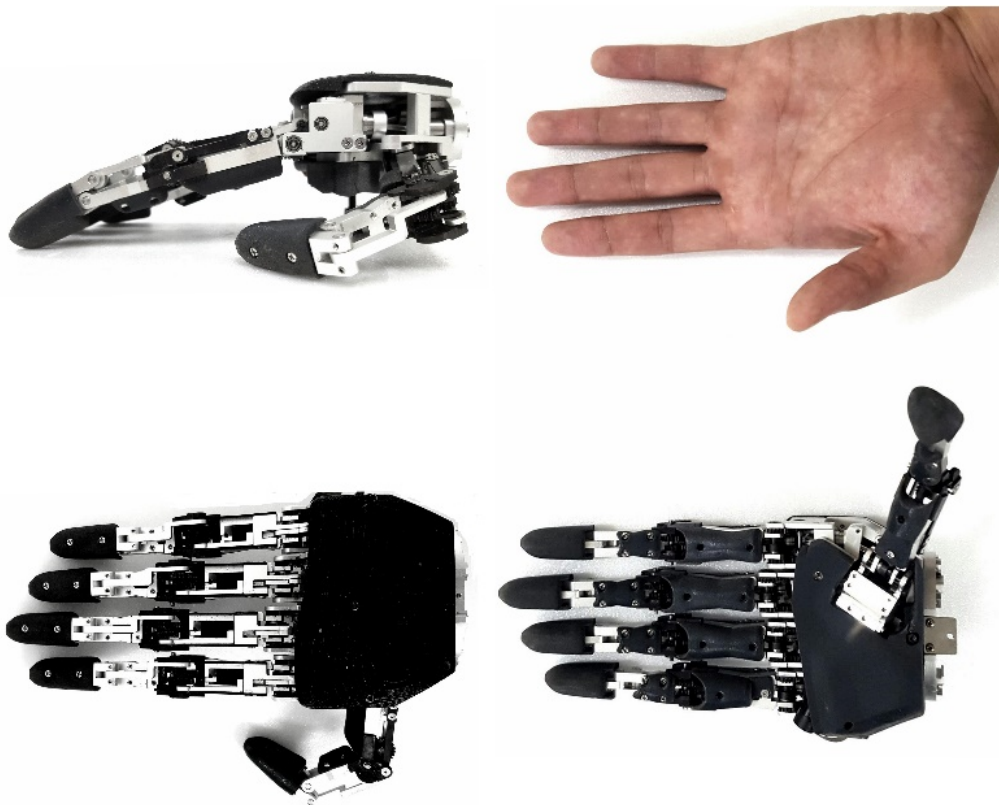
Figure 7. Prototype of the developed prosthetic hand and size comparison with a human hand.

Table 2. Specifications of the developed prosthetic hand.

Weight	475 g		
Overall size [length, width, thickness]	[175 mm, 82 mm (palm), 44 mm]		
Finger sizes [length, width, thickness]	Thumb	[120 mm, 18 mm, 11 mm]	
	Index finger		
	Middle finger		
	Ring finger		
	Little finger		
Degrees of freedom	20		
Active motions	5		
Passive motions	15		
Joint coupling method	Gears and linkages		
Adaptive grasping	Yes		
Ranges of motion	Extension/Flexion	DIP joint	0–90°
		PIP joint	0–90°
		MCP joint	0–108°
	Adduction/Abduction		0–10°
	Passive motion of thumb		0–50°
	Adaptive grasping in PIP and MCP joints		0–25°
Finger/Grasp speed		DIP joint	152.28°/s
		PIP joint	304.56°/s
		MCP joint	487.30°/s

DIP: distal interphalangeal, PIP: proximal interphalangeal, and MCP: metacarpophalangeal.

The white and black linkages in Figure 7 were manufactured from aluminum 6061 and steel, respectively, considering strength and deflection. To satisfy the desired specifications, the diameter of the coil and internal diameter of the torsional spring were 1 mm and 6 mm, respectively. Furthermore, the actuator offered by Maxon Motor has a gearbox with 256:1 ratio, and the output rpm and torque are 25.43 rpm 0.39 Nm, respectively. We controlled each actuator at its current mode control. Because of the use of the actuator with 25.43 rpm, the distal, middle, and proximal phalanges move at 152.28, 304.56, 487.30°/s, respectively. The grasp speed (152.28°/s) was designed to be over the minimal acceptable speed (115°/s) suggested in [2]. The specifications of the developed prosthetic hand are summarized in Table 2.

4.2. Experiment

The experiments to verify the functionality of the prosthetic hand were performed in two sections. The experiments in each section were organized to verify the performance of the developed hand mechanism and to check usability when a patient uses the prosthetic hand.

In the experiment of the first section, the prosthetic hand was fixed on the base involving the actuators. Then, in current control mode, self-adaptive grasping motion was tested, as shown in Figure 8. Using objects with diverse shapes used in daily life, such as a paper cup and a remote control, the prosthetic hand was able to grasp the objects stably.
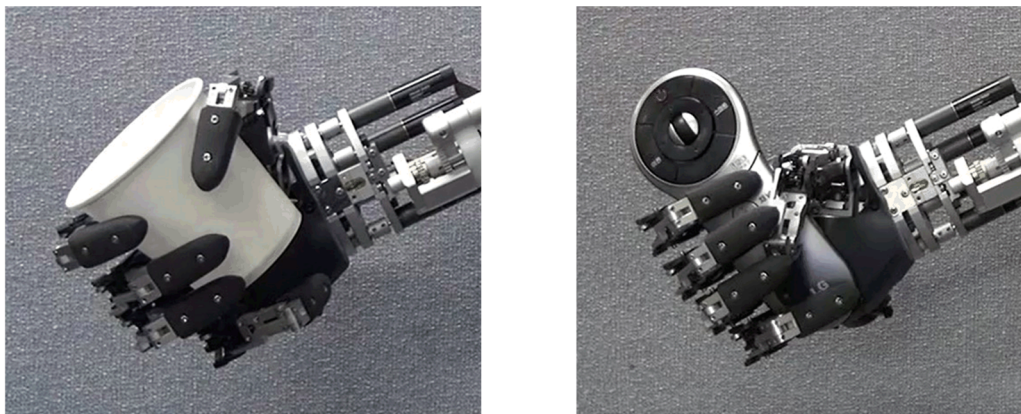

Figure 8. Self-adaptive grasping motions using diverse objects.

In the experiment of the second section, a patient wore the prosthetic hand, and he performed various tasks such as grasping objects and pushing buttons. As shown in the upper pictures in Figure 9, the patient could brush his hair and eat cereal by grasping a hair brush and spoon, respectively. Furthermore, he could surf the internet and change the channel of a television by pushing computer mouse and remote control buttons. From these experiments, the practical applicability of the prosthetic hand was demonstrated using diverse objects encountered in daily life. However, although the weight of the prosthetic hand was 475 g, the patient felt fatigue and discomfort over extended periods of usage.
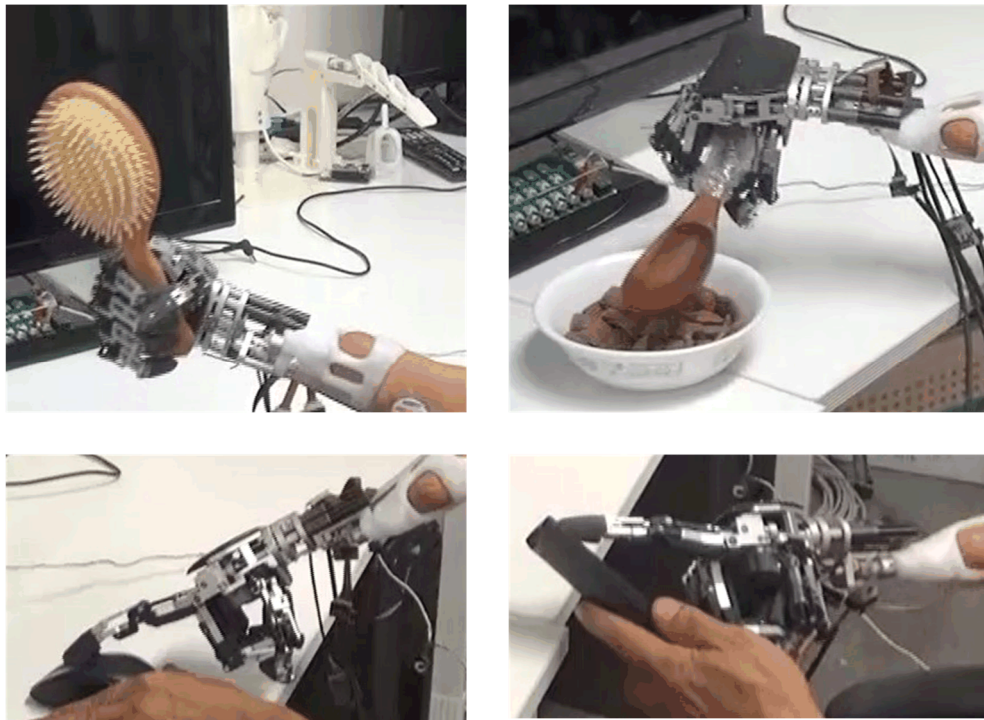
Figure 9. Performance of diverse tasks by a patient: grasping a hair brush and spoon (**upper**) and pushing computer mouse and remote control buttons (**lower**).

5. Conclusions

In this paper, we developed an anthropomorphic prosthetic hand for wrist or forearm amputees. The hand was designed mechanically in an underactuated system to realize grasping motions. In this paper, we also suggested a new method for designing couple joints in an underactuated system. By using two four-bar linkages composed of a combination of linkages and gears, the positions of each phalanx were analyzed accurately, and the sustainability of performance and available payload were improved. Torsional springs installed between coupled joints realized passive motions for self-adaptive grasping. In addition, by using CV joints, the torque produced from the outside can be transferred to finger modules regardless of adduction/abduction motions. From these two main design concepts, the hand has the advantages of a linkage mechanism and can be designed with a more compact weight and size than other published hands. The final design of the developed hand has a weight of 475 g and a normal human hand size of 175 mm. The prosthetic hand realizes self-adaptive grasping, adduction/abduction, and natural motions such as flexion and extension. The hand's fundamental grasping performance on everyday objects was verified experimentally. In further works, we will perform in-depth experiments with diverse subjects and complex tasks in order to improve its comfort and functionality. We also have a plan to make the prosthetic hand lighter by analyzing which parts can be replaced by light material and fabricating the parts using 3D printing.

References

1. Clement, R.G.E.; Bugler, K.E.; Oliver, C.W. Bionic prosthetic hands: A review of present technology and future aspirations. *Surg. J. R. Coll. Surg. Edinb. Irel.* **2011**, *9*, 336–340. [CrossRef] [PubMed]

2. Belter, J.T.; Segil, J.L.; Dollar, A.M.; Weir, R.F. Mechanical design and performance specifications of anthropomorphic prosthetic hands: A review. *J. Rehabil. Res. Dev.* **2013**, *50*, 599–618. [CrossRef] [PubMed]

3. Butterfass, J.; Fischer, M.; Grebenstein, M.; Haidacher, S.; Hirzinger, G. Design and experiences with DLR hand: II. In Proceedings of the World Automation Congress, Seville, Spain, 28 June–1 July 2004; Volume 15, pp. 105–110.

4. Lovchik, C.; Diftler, M. The Robonaut hand: A dexterous robot hand for space. In Proceedings of the IEEE International Conference on Robotics and Automation, Detroit, MI, USA, 10–15 May 1999; Volume 2, pp. 907–912.

5. Jing, X.; Yong, X.; Tian, L.; Togo, S.; Jiang, Y.; Yokoi, H.; Li, G. Development of Tendon Driven Under-Actuated Mechanism Applied in an EMG Prosthetic Hand with Three Major Grasps for Daily Life. In Proceedings of the IEEE/RSJ International Conference on Intelligent Robots and Systems (IROS), Madrid, Spain, 1–5 October 2018.

6. *Touch Bionics Web Site [Internet]*; Touch Bionics Inc.: Mansfield, MA, USA, 2013. Available online: http://www.touchbionics.com/ (accessed on 15 May 2020).

7. *Steeper Group Web Site [Internet]*; RSL Steeper: Leeds, UK, 2013. Available online: http://www.steepergroup.com/ (accessed on 15 May 2020).

8. *Vincent Systems [Internet]*; Vincent Systems: Weingarten, Germany, 2013. Available online: http://vincentsystems.de/ (accessed on 20 May 2020).

9. *Michelangelo Operation Manual*; Otto Bock: Duderstadt, Germany, 2012.

10. Cipriani, C.; Zaccone, F.; Stellin, G.; Beccai, L.; Cappiello, G.; Carrozza, M.C.; Dario, P. Closed-loop controller for a bio-inspired multi-fingered underactuated prosthesis. In Proceedings of the IEEE International Conference on Robotics and Automation (ICRA), Orlando, FL, USA, 15–19 May 2006; pp. 2111–2116.

11. Cipriani, C.; Controzzi, M.; Carrozza, M.C. The smarthand transradial prosthesis. *J. Neuroeng. Rehabil.* **2011**, *8*, 29. [CrossRef] [PubMed]

12. Dechev, N.; Cleghorn, W.; Naumann, S. Multiple finger, passive adaptive grasp prosthetic hand. *Mech. Mach. Theory* **2001**, *36*, 1157–1173. [CrossRef]

13. Akella, P.N.; Cutkosky, M.R. Contact Transition Control with Semiactive Soft Fingertips. *IEEE Trans. Robot. Autom.* **1995**, *11*, 859–867. [CrossRef]

14. Prattichizzo, D.; Mercorelli, P.; Bicchi, A.; Vicino, A. On the geometric control of internal forces in power grasps. In Proceedings of the IEEE Conference on Decision and Control, San Diego, CA, USA, 12 December 1997; Volume 2, pp. 1942–1947.

15. Cutkosky, M.R. On Grasp Choice, Grasp Models, and the Design of Hands for Manufacturing Tasks. *IEEE Trans. Robot. Autom.* **1989**, *5*, 269–279. [CrossRef]

16. Kim, T. Design of 2-Axis Adaptive Fingered Gripper Using Spherical Five-Bar Linkage. Master's Thesis, Department of Mechanical Engineering, Yonsei University, Seoul, Korea, 2014; p. 9.